2011 IEEE International Conference on Robotics and Automation
Shanghai International Conference Center
May 9-13, 2011, Shanghai, China

Design and Control of an Actuated Thumb Exoskeleton for Hand Rehabilitation Following Stroke

Furui Wang, Milind Shastri, Christopher L. Jones, Vikash Gupta,
Christian Osswald, Xuan Kang, Derek G. Kamper, and Nilanjan Sarkar

Abstract— **Chronic hand impairment is common following stroke. This paper presents an actuated thumb exoskeleton (ATX) to facilitate research in hand rehabilitation therapy. The ATX presented in this work permits independent bi-directional actuation in each of the 5 degrees-of-freedom (DOF) of the thumb using a mechanism that has 5 active DOF and 3 passive DOF. The ATX is able to provide considerable joint torques for the user while still allowing backdrivability through flexible shaft transmission. A prototype has been built and experiments were conducted to evaluate the closed-loop position control. Further improvement and future work are discussed.**

I. Introduction

Hand impairment is a prevalent outcome for a variety of neuromuscular disorders, such as stroke. Up to 795,000 people in the U.S. experience a stroke each year [1]. Of these, 60-75% will live beyond one year after the incidence, resulting in a current stroke population of 6.5 million [1]-[2]. Arm function is acutely impaired in a large majority of those diagnosed with stroke [3]-[5]. Furthermore, acute hemiparesis presages chronic hemiparesis in over 40% of individuals [3], [4]. Chronic deficits are prevalent in the distal upper extremities, especially with regard to finger extension [6].

This distal limb impairment can be especially disabling, as proper hand function is crucial to manual exploration and manipulation of the environment. Indeed, loss of hand function due to neuromuscular disorders frequently prevents effective self-care and limits employment opportunities. One study reported that more than half of the subjects they observed were dependent on others for help in the activities of daily living six months post-stroke [7].

An assortment of interventions has been tried in an effort to improve function or to treat the resulting peripheral alterations following stroke. Those with the most success to date tend to focus on repetitive practice. Indeed numerous studies employing the constraint-induced technique, in which focus is placed on intensive practice with the impaired arm without using the less impaired arm, have shown improvement in hand capabilities [8]-[9]. This supports the observations in animal models of stroke in which practice appears to be the primary factor leading to synaptogenesis and brain plasticity [10]-[11].

Unfortunately, many stroke survivors do not possess sufficient sensorimotor control to practice the desired movements. For the upper extremity, robots have been created to assist with therapeutic training of the wrist, arm and shoulder [12]-[15]. It has been reported that robot-delivered sensorimotor training enhanced the motor performance of the exercised shoulder and elbow with improved functional outcome [16] and that practicing with a robot that assisted reaching movements helped the users learn how to generate smoother unaided reaching trajectories [17].

In recent years, a number of devices have been developed expressly for or applied to hand rehabilitation. These include both commercial products, such as CyberGrasp (Immersion Corporation, San Jose, CA), the Hand Mentor (Kinetic Muscles Inc., Tempe, AZ) and the Amadeo System (Tyromotion GmbH, Graz, Austria), and experimental devices, such as Rutgers Master II-ND, HWARD and HandCARE, among others [18]-[20].

Questions remain, however, as to how best to use robotic devices to facilitate rehabilitation. Should the device assist or resist movement? Should movement error actually be augmented, as some have suggested [21]? Should emphasis be placed on practice of movement of individual joints [22] or on the coordination of multiple joints?

The majority of the systems developed for the hand do not allow for independent control of each DOF of the finger/thumb joints, making it difficult to answer these questions. This is especially true for the thumb, which is typically modeled with five degrees-of-freedom (DOF) [23]-[24]. An 18 DOF hand device has been developed in Japan for hand and wrist rehabilitation following stroke [20]. This device actuates 4 DOF for the thumb. The joint torques that it can provide, however, are limited to roughly 0.3 N-m, a value that may not be sufficient for resistive or perturbation therapy paradigms.

Thus, in this work, we are designing an actuated thumb exoskeleton (ATX) with 5 active DOF that allows independent actuation of each DOF of the thumb. The ATX is able to provide considerable torque to overcome the excessive coactivation or increased stiffness in the affected thumb. We present our first prototype of the ATX and initial experimental results in this paper. The paper is organized as follows: Section II describes the mechanical design of the ATX; Section III presents the kinematic analysis; Section IV introduces the real-time control system; Section V shows the instrumentation and initial experimental results; and Section VI discusses the necessary improvement and Section VII concludes the paper and proposes future work.

Furui Wang, Milind Shastri, Vikash Gupta and Nilanjan Sarkar are with the Department of Mechanical Engineering, Vanderbilt University, Nashville, TN, 37212, USA (email: {furui.wang, vikash.gupta, milind.shastri, nilanjan.arkar}@Vanderbilt.edu).

Christopher L. Jones, Christian Osswald and Xuan Kang are with the Department of Biomedical Engineering, Illinois Institute of Technology, Chicago, IL, 60616, USA (email: jonechr@Iit.edu, cosswald@iit.edu, xuankang@hotmail.com,).

Derek G. Kamper is with the Department of Biomedical Engineering, Illinois Institute of Technology and the Rehabilitation Institute of Chicago, Chicago, IL, 60611, USA (e-mail: d-kamper@northwestern.edu).

II. The ATX Design

The design of the ATX presented in this paper has the following considerations:

A. Independent actuation of each thumb DOF

In recent literature, the human thumb has been generally modeled as a five DOF manipulator with the virtual links connected by revolute joints, in accordance with anatomical models of the thumb [23]-[24]. The 5 DOF are: flexion/extension (F/E) of the carpometacarpal (CMC) joint followed by abduction/adduction (Ab/Ad) of the CMC joint, then Ab/Ad followed by F/E of the metacarpophalangeal (MCP) joint, and finally by F/E of the interphalangeal (IP) joint. Consecutive rotational axes may be non-orthogonal and non- intersecting. The orientation of the axes of rotation in the thumb model follows the anatomical descriptions (Fig. 1). The anatomy-based kinematic model of the thumb has been converted into a robotics-based description with the standard Denavit-Hartenberg (D-H) parameters in [24], thus, it is possible to approximate thumb kinematics using an exoskeleton with hinged linkages.

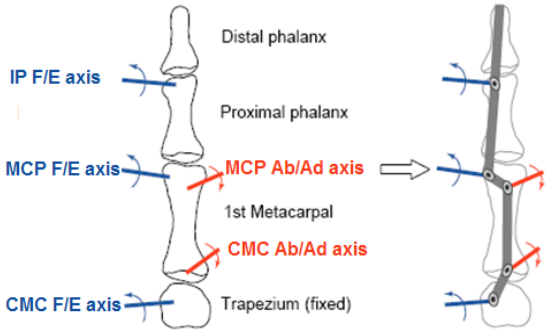

Fig. 1 A Virtual Five-link Model of the Thumb [24].

In order to achieve independent control of each thumb joint, the ATX presented in this paper has 5 active DOF and 3 Passive DOF. The five active joints produce F/E of the CMC, MCP and IP joints, and Ab/Ad of the CMC and MCP joints (Fig. 2). The exoskeleton physically attaches to the distal, proximal, and metacarpal segments of the thumb. The attachment points which actuate the MCP and IP joints are connected through two-bar linkages, which accommodate the variation in segment lengths across the population. The F/E and Ab/Ad of the CMC joint are directly actuated; the rotational axes of the ATX can be adjusted to align them with the axes of the user (Fig. 2). Note that because the thumb joints are non-orthogonal and non-intersecting, a twisting motion will be observed between the metacarpal and proximal segments when MCP Ab/Ad occurs. Thus a universal joint, which has 2 passive DOF, is developed for the thumb exoskeleton to allow this twisting motion (Fig. 3). This motion is important for thumb opposition.

The thumb and ATX can be modeled as chains of rigid links as shown in Fig. 4. Both the thumb and the ATX models have individually kinematical redundancy for the 3 DOF of their tip locations, as the thumb model has 5 DOF and the ATX has 5 active DOF and 3 passive DOF in the joint-space (orientation of the tips is not considered for the current application). Thus, for a given task-space trajectory, there will be an infinite number of possible joint-space trajectories for both the thumb and the ATX. However, since the thumb and the ATX are coupled by the position constraints at the attachment points, a unique mapping can be achieved between the degrees of freedom of the thumb and the ATX leading to the redundancy of the coupled system the same as that of the thumb alone. So the joint-space trajectories of the thumb can be determined by the joint-space trajectories of the ATX and vice versa. The kinematics of the coupled system of the thumb model and the ATX model has been analyzed in [25]. The result of the kinematic analysis shows that a unique mapping is obtained between the joint-space trajectories of the thumb model and the ATX model.

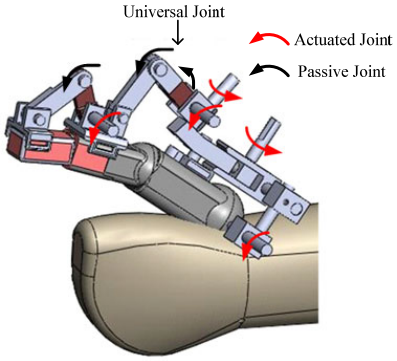

Fig. 2 Solidworks Model of the Thumb Exoskeleton

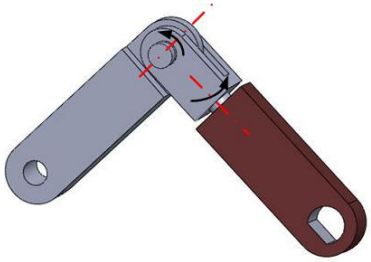

Fig. 3 The Universal Joint between CMC and MCP joints

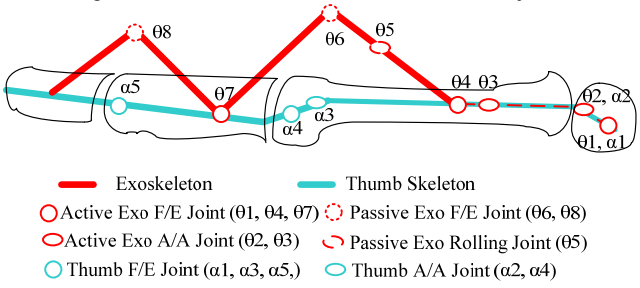

Fig. 4 The simplified thumb and ATX models

B. Joint torque requirement

In order to estimate the output torques of the actuators for the thumb exoskeleton, experiments were carried out to gauge the maximum forces generated at the thumb-tip by stroke survivors and neurologically intact individuals. Nine subjects with severe hand impairment and nine subjects with moderate hand impairment, as rated by the Stage of Hand section of the Chedoke-McMaster Stroke Assessment [26] participated, along with ten control subjects.

In the experiments, subjects were required to generate isometric thumb-tip force in 6 intended directions: distal/proximal, adduction/abduction, flexion/extension (Fig. 5). The configuration of the thumb posture was 50° for CMC extension, 20° for CMC abduction, 20° for MP flexion, 10°

for MCP Abduction and 30° for IP flexion. Details of the experimental setup and procedure are in preparation for a separate publication. The experiment was approved by the Institutional Review Board of Northwestern University.

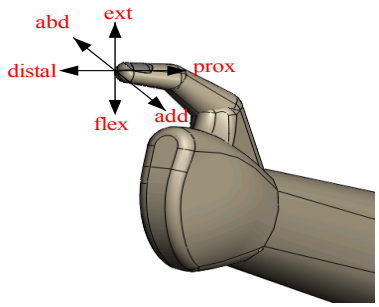

Fig. 5 Directions of Applied Thumb-tip Force

The measured thumb-tip forces were converted into joint torques using

$$\vec{\tau} = J^{T} \cdot \vec{f} \qquad (1)$$

Here, $\vec{\tau} \in \Re^{5\times1}$ is the vector of joint torques; J is the Jacobian matrix of the thumb model; $\vec{f} \in \Re^{3\times1}$ is the vector of the thumb-tip force recorded by the force. The D-H parameters used in the Jacobian matrix were obtained from literature (Table 1). Table 2 shows the maximum torque calculated for each joint for all subject groups.

Table 1 D-H parameters for the thumb model [24]

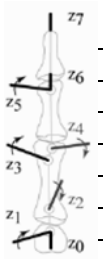

	θ	d (cm)	a (cm)	α (degree)
Z_6 to Z_7	0	3.42	0.03	0
Z_5 to Z_6	θ_5	-0.71	0	94.89
Z_4 to Z_5	θ_4	-1.16	3.99	106.43
Z_3 to Z_4	θ_3	0.85	0.31	-110.37
Z_2 to Z_3	θ_2	0.51	4.45	88.41
Z_1 to Z_2	θ_1	0.21	1.31	-86.86
Z_o to Z_1	0	0.59	-0.12	-93.86

Table 2 Calculated Maximum Joint Torques of the Thumb (N-m)

Thumb Joint	Subjects		
	Control	Stroke - Moderate	Stroke - Severe
CMC F/E	5.59	2.66	0.99
CMC Ab/Ad	-4.81	-2.40	-0.91
MCP F/E	3.67	1.54	0.94
MCP Ab/Ad	-3.09	-1.78	-0.85
IP F/E	1.85	0.58	0.48

To accommodate the majority of our target population, we chose the peak joint torque outputs of the exoskeleton to be comparable to those of moderate stroke subject, which are 2.5 N-m at CMC F/E and Ab/Ad joints, 1.5 N-m at MCP F/E and Ab/Ad joints, 0.5 N-m at IP F/E joint.

C. Actuation System

The ATX is actuated by electric motors. To minimize the weight of the exoskeleton carried by the user, the motors are located remotely from the thumb exoskeleton, and supported by an external platform. This is made possible by the use of flexible shafts to transmit motor torque to the ATX. The flexible shaft, coupled to both the motor shaft and the driving shaft on the thumb exoskeleton joint (Fig. 6), transmits rotary motion between the motors and the exoskeleton while allowing flexibility in its shape between its two ends. The flexible shaft can change shape to accommodate variations in distance between the motor and the exoskeleton as the digit moves. This flexibility makes the system backdrivable. As the shaft provides a rigid coupling, it can rotate the joint in either clockwise or counter-clockwise direction and, thus, only one motor is needed for each DOF. A semi-rigid tube is used as a casing to restrict the curvature of the flexible shaft and prevent it from helixing during the transmission of torque.

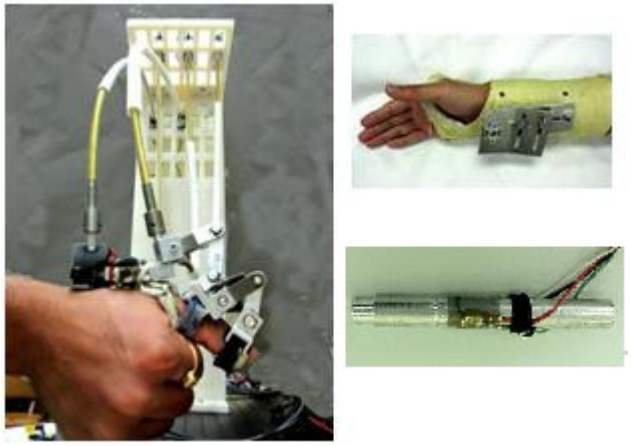

Fig. 6 The ATX with flexible shafts. For a better view of the ATX, the forearm attachment (right top) on which the ATX is fixed is not shown in the picture on the left. Right bottom: strain gage sensor for torque measurement.

D. Integrated Sensor System

Joint angles and torques are measured directly at the joints of the ATX. The joint angles are measured by potentiometers (Precision Electronics Corp., Toronto, Canada) affixed to the shafts of the ATX with gear sets. The motors also have integrated encoders, however, due to the flexible shaft transmission, the values measured at the motor shafts and the ATX shafts may deviate. The deviation between the two measurements can be used to detect mechanical failure. The joint angles of the thumb can be calculated by the joint angles of the ATX through kinematic equations.

Joint torques are measured through full-bridge strain gages attached on the cylindrical driving shafts of the ATX. The strain gage torque measurement has been calibrated and the hysteresis is negligible.

E. The Real-time Control System

The real-time control system of the ATX was developed using MATLAB xPC target software [27]. The xPC target is a real-time environment that consists of a target PC for running real-time applications. The control system consists of two parts: a host PC with MATLAB Simulink software, to create the controller model using Simulink blocks and then compile the model to the executable code; and a target PC running the xPC Target real-time kernel, which downloads the executable code from the host PC and runs it in real-time. The data signals acquired by the target PC are uploaded to the host PC over a direct crossover Ethernet cable. The experimenter monitors the data signal in the host scope and tunes the parameters online in the Simulink model created in the host PC.

A PCI-6229 ADC board (National Instruments) is installed on the target PC to perform analog-digital conversion of torque sensor signals and potentiometer signals. A

PCIM-DDA06/16 DAC board (Measurement Computing) sends analog control commands to the motor amplifiers. All signals are sampled at 1 kHz.

F. Safety and Limitations

A number of safety mechanisms are implemented to ensure safe interaction with the individual's hand. The lever linkages restrict the angular position of each joint of the ATX in the acceptable range. An emergency kill switch is provided to immediately disable all motors. Software monitoring of both position and motor torque, will continuously check to see if specified limits are exceeded and will immediately disable the system should this occur.

III. Instrumentation and Experimental Results

A. Flexible Shaft Tests

In our design, the torque transmission through the flexible shafts allows the actuators to be placed remotely from the ATX. Our major concerns regarding the flexible shaft transmission are the off-axis forces/torques in unintended directions and the helixing of the shaft under high load. Preliminary tests were performed to investigate the transmission performance of the flexible shafts with different input torques (Fig. 7). The flexible shaft was bent with a 90° curvature in the tests. Bending with this curvature had been tested to render good flexibility at its two ends. The flexible shafts in the ATX use the same curvature.

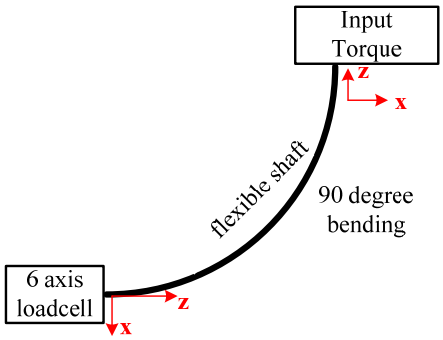

Fig. 7 Schematics of Flexible Shaft Tests

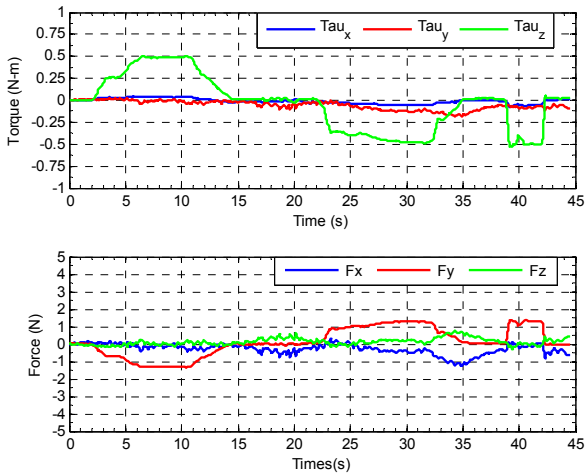

Fig. 8 Off-axis force/torque with 90° shaft bending under low input torque

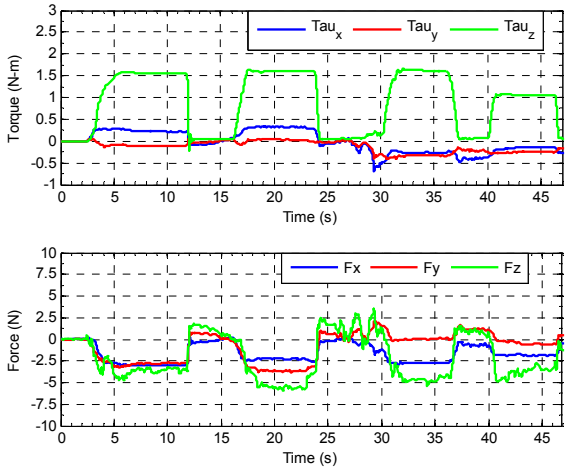

Fig. 9 Off-axis force/torque with 90° Shaft Bending under high torque

Fig. 8 and Fig. 9 show the experimental results of the tests. When the input torque manually applied along the shaft axis (i.e., z-axis) was low (up to 0.5 N-m), which was sufficient for free motion, the off-axis forces and torques in other directions were minimal (<1.5N, Fig. 8). When the input torque was increased to around 1.5 N-m (the maximum torque required for the MCP and IP joints of the ATX), the maximum off-axis force was about 6N, directed along the z-axis, and the maximum off-axis torque was less than 0.3 N-m, about the x-axis. No significant helixing of the flexible shafts was observed during the experiments; the outside semi-rigid casing was able to prevent the undesired movement of the flexible shaft.

B. Closed-loop Joint Position Control

To evaluate the actuation and transmission system of the ATX, experiments were conducted to perform closed-loop joint position control with PID controller on a healthy subject. The feedback signal to the PID controller was the joint angle of the thumb calculated from the joint angle of the ATX, as measured with the potentiometer. The ATX is currently actuated by RC servo motors for testing purpose.

The first experiment was to track a step target with the amplitude of 45 degree in flexion of the IP joint (Fig. 10). The subject passively followed the actuation from the ATX. The control gains of the PID controller were tuned to achieve faster response. The tracking performance was quite good. The steady state error was less than 1 degree and the actual position was able to reach the target position in 0.5 second. A small delay was observed at the beginning of the tracking, possibly due to the response time of the servo motor.

The second experiment was to track a sinusoidal target trajectory with the amplitude of 30 degree and angular frequency of π (Fig. 11) for the IP joint. The subject again passively followed the actuation from the ATX. The tracking of the sinusoidal target was quite good. The correlation factor between the actual and target position was 0.9878. Phase delay was observed near the peak spots of the sinusoidal wave. It might be caused by the unwinding and preloading of the flexible shaft when the rotary direction changed. The response time of the servo motor might also contribute to this delay.

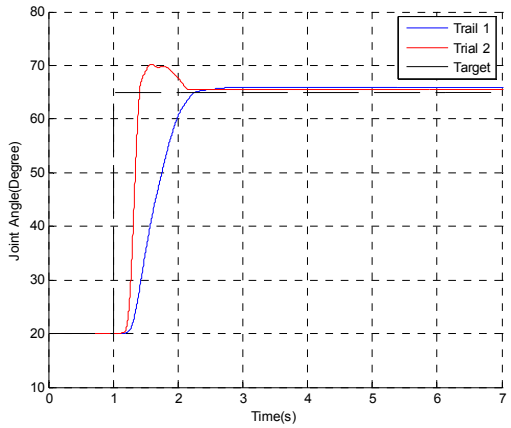

Fig. 10 Step target tracking performance with different control parameters

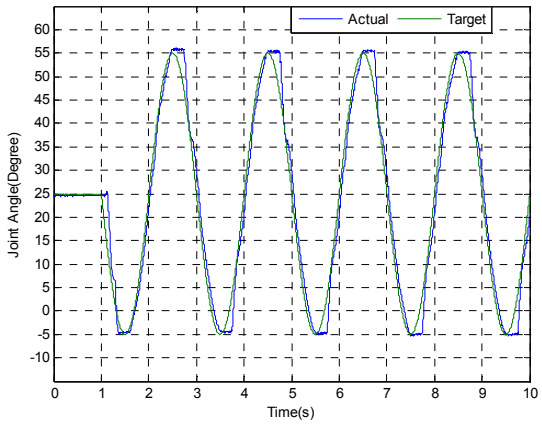

Fig. 11 Sinusoidal target tracking performance

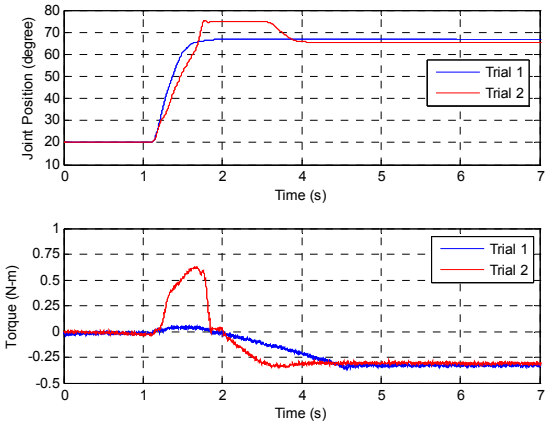

Fig. 12 Joint position and torque when the user passively followed (Trial 1) or actively resisted (Trial 2) the ATX. The motion was in the horizontal plane so the ATX needed to provide extra torque to compensate for the gravity and also friction at the end.

In the third experiment, we repeated the first experiment while in Trial 1 the user did not work against and only passively followed the ATX, and in Trial 2 the user actively worked against the ATX. An overshoot and higher torque were observed in Trial 1 (Fig. 12).

IV. Discussion

To provide a general test-bed for evaluating various training strategies in hand rehabilitation, we are designing a thumb exoskeleton which provides independent actuation of each thumb joint. The first prototype of the designed ATX is able to produce the natural motion of the thumb, which is modeled as a 5 DOF manipulator with virtual linkages connected by non-orthogonal and non-intersecting revolute joints based on the anatomical model [23]-[24]. The total weight of the exoskeleton is less than 200 grams.

In the next step, minor adjustments, e.g., the lengths of the linkages, the size of the thumb attachments, and the diameters and lengths of flexible shafts, will be made to reduce the size of the ATX and improve efficiency of the mechanism.

The sensory system with potentiometer and strain gage is able to provide angular position and torque feedback. The angular position feedback has been used in the closed-loop control in our experiments.

Flexible shafts are used in the transmission system, which allow the backdrivability of the ATX. Testing of torque transmission through flexible shafts showed that off-axis forces/moments generated by flexible shafts were quite small, less than 1.5 N in off-axis force and 0.15 N-m in off-axis torque, under low torque input (0.5 N-m). This low torque input is actually sufficient to drive the voluntary motion of the ATX and human thumb. While under high torque input (1.5 N-m), the maximum off-axis force is about 6N, and the maximum off-axis torque is around 0.4 N-m. Note that this high torque is only needed when the user applies force on an object or has exceptionally high stiffness in the thumb joint. In such cases, the effect of off-axis forces and moments will be minimized due to the structural rigidity of the thumb.

It should be noted, that torque losses are present in the flexible shaft transmission such that the torque generated at motor is not all transmitted to the exoskeleton. This necessitates the measurement of torque directly at the joint. This is achieved in our design by placing strain gages directly on the drive shaft of the exoskeleton. Potentiometers located at the drive shafts provide feedback of joint angle. The angular position feedback has been used in the closed-loop control in our experiments. Closed-loop control of force will be developed next.

The ATX is currently actuated by RC servo motors. For testing of mechanical design and actuation system, RC servo motors are cost-effective alternatives compared with DC motors. With closed-loop position control, the IP joint is able to achieve accurate performance in the experiments. The steady-state error of closed-loop position control was less than 1 degree in the step target tracking. Considering the flexibility of thumb skins and possible slippage at attachment points, this control performance was satisfying. In the sinusoidal target tracking, the tracking performance was quite good with a correlation factor of 0.9878. Delays in the system response were observed at certain spots, however, especially when the ATX started to move or to change rotary directions. The use of servo motors, which has inherited response delay about 0.1 seconds, would have slowed down the overall response. The transmission by flexible shafts might have also contributed to the delay as flexible shafts would wind/unwind and preload when the actuation started or changed directions. This response time of the system will be further quantified with Kollmorgen AKM DC motors that have faster response and higher speed and torque. Our goal is to achieve a

bandwidth of 2 Hz or more for the actuation system. In the third experiment, the ATX worked against the resistance from the user and still showed controllability and stability. An overshoot was observed as expected after the user reduced the resistance but the error decreased to normal range after a short period.

From the experimental results and analysis, we believe that the current design meets our design requirements and is able to provide controllable independent actuation to each thumb joint with sufficient torque. The transmission through flexible shafts is a viable solution.

V. Conclusion and Future Work

This paper presents the design and first prototype of an actuated thumb exoskeleton (ATX) that permits independent bi-directional actuation in each of the 5 DOF of the thumb using a mechanism that has 5 active DOF and 3 passive DOF. The transmission system using flexible shaft is able to transmit considerable amount of joint torques for the user while still allowing backdrivability. Independent control of each thumb joint and the ability to provide sufficient torque to overcome the excessive coactivation or increased stiffness in the affected hand are the important criteria in designing a test-bed to facilitate research in hand rehabilitation therapy. Experiments of closed-loop position control were conducted and the tracking performance of a step target and a sinusoidal target showed good controllability with the sensory feedback.

In the future work, we will implement the position control for all 5 active joints of the ATX and enhance the ATX with different operation modes, e.g., passive mode, active mode and assist-as-needed mode.

The ATX will be coupled with an actuated finger exoskeleton (AFX) [28] that we have developed for the index finger to provide a test bed for evaluating rehabilitation strategies in restoring control of pinch and reach-to-pinch movements following stroke.

Acknowledgment

This work is partially supported by NIH grants R24HD050821 and 5 R21HD055478-02. We acknowledge Mr. Roderick Keith from KMW Inc. for the helpful feedback during the fabrication of the exoskeleton.

References

[1] American Heart Association: Heart and Stroke Statistical Update, http://www.Americanheart.org/statistics/stroke.htm, 2009.

[2] J. P. Broderick, S. J. Phillips, J. P. Whisnant, W. M. O'Fallon, and E. J. Bergstralh, "Incidence rates of stroke in the eighties: the end of the decline in stroke?," Stroke, vol. 20, pp. 577-582, 1989.

[3] C. S. Gray, J. M. French, D. Bates, N. E. Cartlidge, 0. F. James, and G. Venables, "Motor recovery following acute stroke," Age Ageing, vol. 19, pp. 179-84, 1990.

[4] H. Nakayama, H. S. Jorgensen, H. 0. Raaschou, and T. S. Olsen, "Recovery of upper extremity function in stroke patients: The Copenhagen Stroke Study," Arch Phys Med Rehabilitation, vol. 75, pp. 394-398, 1994.

[5] V. M. Parker, D. T. Wade, and R. Langton Hewer, "Loss of arm function after stroke: measurement, frequency, and recovery." Int. Rehab Med, vol. 8, pp. 69-73, 1986.

[6] C. A. Trombly, "Stroke," in Occupational Therapy for Physical Dysfunction, Baltimore: Williams and Wilkins, 1989, pp. 454-471.

[7] D. Wade, "The epidemiologically based needs assessment reviews." Health Care Needs Assessment, Volume I, J. Raftery, Ed., 1994, pp. 111-255.

[8] S. L. Wolf, S. Blanton, H. Baer, J. Breshears, and A. J. Butler, "Repetitive task practice: a critical review of constraint-induced movement therapy in stroke," Neurologist, vol. 8, pp. 325-3 8, 2002.

[9] S. J. Page, S. Sisto, P. Levine, and R. E. McGrath, "Efficacy of modified constraint-induced movement therapy in chronic stroke: a single-blinded randomized controlled trial," Arch Phys Med Rehab, vol. 85, pp. 14-8, 2004.

[10] T. A. Jones, C. J. Chu, L. A. Grande, and A. D. Gregory, "Motor skills training enhances lesion-induced structural plasticity in the motor cortex of adult rats," JNeurosci, vol. 19, pp. 10153-63, 1999.

[11] J. A. Kleim, T. A. Jones, and T. Schallert, "Motor enrichment and the induction of plasticity before or after brain injury," Neurochem Res, vol. 28, pp. 1757-69, 2003.

[12] L. R. Macclellan, D. D. Bradham, J. Whitall, B. Volpe, P. D. Wilson, J. Ohlhoff, C. Meister, N. Hogan, H. I. Krebs, and C. T. Bever, Jr., "Robotic upper-limb neurorehabilitation in chronic stroke patients," J Rehabil Res Dev, vol. 42, pp. 717-22, 2005.

[13] M. Ferraro, J. J. Palazzolo, J. Krol, H. I. Krebs, N. Hogan, and B. T. Volpe, "Robot-aided sensorimotor arm training improves outcome in patients with chronic stroke," Neurology, vol. 61, pp.1604-7, 2003.

[14] P. S. Lum, C. G. Burgar, P. C. Shor, M. Majmundar, and M. Van der Loos, "Robot-assisted movement training compared with conventional therapy techniques for the rehabilitation of upperlimb motor function after stroke," Arch Phys Med Rehabil, vol. 83, pp. 952-9, 2002.

[15] Gupta, A., O'Malley, M. K., Patoglu, V. and Burgar, C., "Design, control and performance of RiceWrist: a force feedback wrist exoskeleton for rehabilitation and training" The International Journal of Robotics Research, 27, 233-251, 2008.

[16] B. T. Volpe, H. I. Krebs, N. Hogan, 0. L. Edelstein, C. Diels, and M. Aisen, "A novel approach to stroke rehabilitation: robotaided sensorimotor stimulation," Neurology, vol. 54, pp. 1938- 44, 2000.

[17] L. E. Kahn, M. L. Zygman, W. Z. Rymer, and D. J. Reinkensmeyer, "Effect of robot-assisted and unassisted exercise on functional reaching in chronic hemiparesis," presented at 23rd Annual IEEE Engineering in Medicine and Biology Conference, Istanbul, Turkey, 2001.

[18] A. Wege and G. Hommel, "Development and control of a hand exoskeleton for rehabilitation of hand injuries," IEEE/RSJ International Conference on Intelligent Robots and Systems, Edmonton, Canada, 2005.

[19] M. DiCicco, L. Lucas, and Y. Matsuoka, "Strategies for an EMG-controlled orthotic exoskeleton for the hand," IEEE International Conference on Robotics and Automation, New Orleans, USA, 2004.

[20] Kawasaki H, Ito S, Ishigure Y, Nishimoto Y, Aoki T, Mouri H, et al. "Development of a hand motion assist robot for rehabilitation therapy by patient self-motion control". IEEE 10th Intl Conf Rehab Rob. Noordwijk, The Netherlands, 2007: 234-240.

[21] J. L. Patton, M. E. Stoykov, M. Kovic, and F. A. Mussa-Ivaldi, "Evaluation of robotic training forces that either enhance or reduce error in chronic hemiparetic stroke survivors," Exp Brain Res, vol. 168, pp. 368-83, 2006.

[22] S. Hesse, C. Werner, M. Pohl, S. Rueckriem, J. Mehrholz, and M. L. Lingnau, "Computerized arm training improves the motor control of the severely affected arm after stroke: a single-blinded randomized trial in two centers," Stroke, vol. 36, pp. 1960-6, 2005.

[23] Giurintano DJ, Hollister AM, Buford WL, Thompson DE, Myers LM. "A virtual five-link model of the thumb", Med Eng Phys 1995; 17: 297-303.

[24] Santos VJ, Valero-Cuevas FJ. "Reported anatomical variability naturally leads to multimodal distributions of Denavit-Hartenberg parameters for the human thumb", IEEE Trans Biomed Eng 2006; 53: 155-63.

[25] Vikash Gupta, "Kinematic analysis of a thumb-exoskeleton system for post stroke rehabilitation", Thesis (M.S. in Mechanical Engineering), Vanderbilt University, Aug. 2010.

[26] Gowland C, Stratford P, Ward M, Moreland J, Torresin W, Van Hullenaar S, Sanford J, Barreca S, Vanspall B, Plews N. Measuring physical impairment and disability with the chedoke-mcmaster stroke assessment. *Stroke*. 1993;24:58-63

[27] xPC target, Mathworks, http://www.mathworks.com/help/toolbox/xpc/

[28] C. Jones, F. Wang, et al, "Control and Kinematic Performance Analysis of an Actuated Finger Exoskeleton for Hand Rehabilitation Following Stroke ", IEEE International Conference on Biomedical Robotics and Biomechatronics, Tokyo, Japan, 2010.